J Mater Sci (2011) 46:3835–3839
DOI 10.1007/s10853-011-5298-x

Magnetic and structural properties of Fe_xPt_{100-x} on MgO(110) substrates

Wei Lu · Junwei Fan · Yuxin Wang · Biao Yan

Received: 9 August 2010 / Accepted: 17 January 2011 / Published online: 29 January 2011

Abstract Fe_xPt_{100-x} ($70.1 \leq x \leq 83.4$) thin films with ordered Fe_3Pt phase were grown successfully onto MgO(110) substrates by electron beam evaporation. The unit cell of ordered Fe_3Pt phase is elongated along *c*-axis direction and the thin films become more chemically ordered with decreasing Fe content. The magnetization of thin films shows a decrease when Fe content is around 79 at.%. The relationship between magnetic anisotropy and structural parameters suggests that the change of magnetic anisotropy in ordered Fe_3Pt thin films with different compositions most likely stems from the magnetocrystalline origin.

Introduction

Fe–Pt alloy systems have drawn much attention due to their interesting properties and potential applications in permanent magnets and recording media [1–9]. Binary Fe–Pt alloys have several ordered phases: cubic Cu_3Au ($L1_2$) structure for Fe_3Pt and $FePt_3$ and CuAu ($L1_0$) structure for FePt. The equiatomic FePt may form chemically ordered compounds of tetragonal $L1_0$ phase which possesses a modulate structure consisting of pure Fe and Pt planes stacked alternately along the tetragonal *c*- (easy) axis, thus resulting in an extremely high uniaxial magnetic anisotropy energy ($K_u \sim 10^7$ J/m^3) [1]. It was reported that Fe_3Pt alloys exhibit many interesting properties such as invar effect, large magneto-volume effect, and shape memory effect [6–9]. On the other hand, in bulk Fe_3Pt alloy, it is known that it exhibits small magnetic anisotropy in both ordered and disordered phases because of cubic crystal symmetry. However, theoretical band structure calculation revealed a strong hybridization of an ordered Fe_3Pt between Fe and Pt *d* state [2, 3] and recently, it was predicted that Fe_3Pt alloy thin films could possess a large in-plane magnetic anisotropy in deforming fcc to fct or m-DO_{19} phase [4]. Experimentally, it was observed that the "quasi" $L1_2$ ordered phase of Fe_3Pt alloy thin films deposited onto MgO(100), (111) single crystal substrates exhibits giant in-plane cubic magnetic anisotropy constants ($K_1 = -4 \times 10^7$, $K_2 = 2 \times 10^6$ J/m^3) at room temperature [5]. For the epitaxial $L1_2$-ordered Fe_3Pt thin films, the magnetic properties (especially magnetocrystalline anisotropy) and the order parameter, i.e., the volume average fraction of atoms on the correct lattice sites, have been determined as a function of substrate temperature and substrate type [5]. However, since the ordering characteristics and the magnetic properties for nonequiatomic composition are different from those for the equiatomic composition, it is of interest to investigate the crystallographic structure and the resultant magnetic properties as a function of alloy composition. In this study, we systematically investigate the compositional dependence on the structure and magnetic properties in Fe_3Pt thin films which is fabricated onto MgO(110) single crystal substrates for the first time. For the Fe_3Pt alloy thin films grown onto MgO(110) single crystal substrate, the magnetic anisotropy, K_1 and K_2, can be obtained at the same time while for the thin films grown onto MgO(100), only K_1 can be obtained and only K_2 can be got for the case of MgO(111) substrate. In addition, the MgO(110) single crystal substrate is chosen in current experiment since we can get the knowledge of magnetic anisotropy of Fe_3Pt alloy thin films with different orientation.

W. Lu (✉) · J. Fan · Y. Wang · B. Yan
School of Materials Science and Engineering, Shanghai Key Lab. of D&A for Metal-Functional Materials, Tongji University, Shanghai 200092, China
e-mail: weilu@tongji.edu.cn

Experimental

The Fe_xPt_{100-x} thin films with Fe content from around 70–85 at.% were fabricated by electron beam evaporation onto MgO(110) single crystal substrates using Fe and Pt elemental targets. The base pressure of the deposition system is around 1×10^{-8} Torr. Before deposition, the substrate was cleaned in acetone by using ultrasonic cleaner for 20 min. The substrate deposition temperature was kept at 550 °C. The deposition rate of thin films is around 0.05 nm/s and the film thickness is about 50 nm. The composition of thin film was analyzed by Shimazu energy dispersive X-ray EDX-700 spectrometer (taking an average of 10 measurements). The structural analysis was performed using a Rigaku high-power X-ray diffraction (XRD) using Cu-Kα radiation ($\lambda = 0.154056$ nm). Magnetic properties were measured by a high sensitive vibrating sample magnetometer (Toyo Co.) and the magnetic anisotropy constants were measured by torque magnetometer (Toyo Co.).

Results and discussions

Crystallographic structure

Figure 1 shows the schematic diagram of crystallographic structure of ordered Fe_3Pt phase and the epitaxial relationship between Fe_3Pt thin film and MgO(110) single crystal substrate, which was obtained from XRD ϕ scan. The lattice mismatch between ordered Fe_3Pt phase (0.374 nm) and MgO(110) substrate (0.423 nm) is about 11%. Figure 2 shows the XRD patterns of Fe_xPt_{100-x} thin films with Fe content from around 70–85 at.% on MgO(110) single crystal substrates. The superlattice peak of (011) of ordered Fe_3Pt phase is observed over a range of 70.1–83.4 at.%. This result indicates that Fe_xPt_{100-x} thin films with ordered Fe_3Pt phase were grown successfully onto MgO(110) substrates at substrate temperature 550 °C. When Fe content is larger than 83.4 at.% (e.g., 85 at.%), the structure is disordered and there is no signal of the

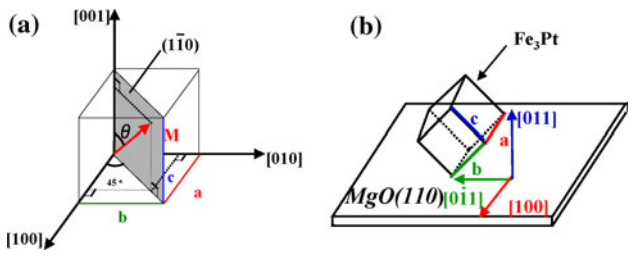

Fig. 1 Schematic diagram of **a** crystallographic structure of ordered Fe_3Pt phase and **b** epitaxial relationship between Fe_3Pt thin film and MgO(110) single crystal substrate

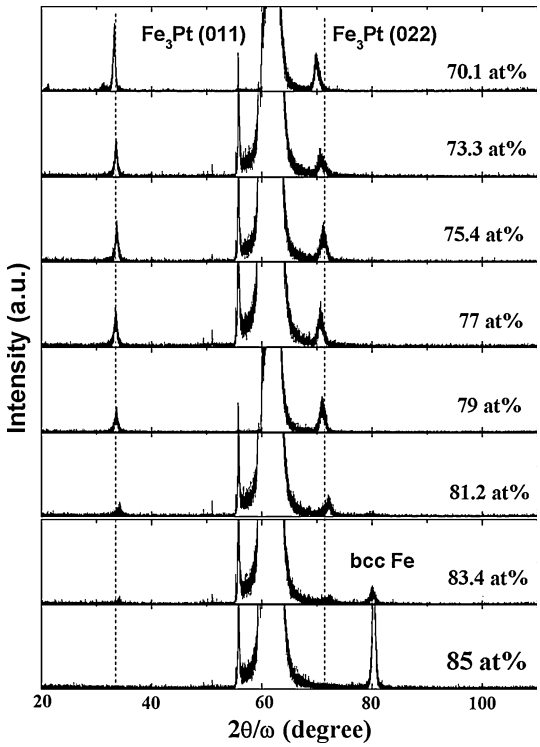

Fig. 2 XRD patterns of Fe_xPt_{100-x} thin films with x from around 70–85 at.%

formation of ordered Fe_3Pt phase. The peak at around 80° in thin films with Fe content larger than 83.4 at.% is contributed by bcc Fe solid solution and the other peaks come from the MgO substrate. In order to determine the in-plane lattice constant, the ϕ scan analysis was performed by XRD. The ϕ scan result (which was not shown here) indicates that the Fe_xPt_{100-x} samples have 2-fold symmetry when $70.1 \leq x \leq 83.4$ and the [011] unit-cell axis of ordered Fe_3Pt phase is perpendicular to the film plane, which agrees well with the epitaxial relationship between Fe_3Pt thin film and MgO(110) single crystal substrate shown in Fig. 1b. According to the XRD analysis, the Fe_3Pt thin films were epitaxially grown onto MgO(110) substrates.

Figure 3 shows the changes of lattice constants a and c of ordered Fe_3Pt phase as a function of Fe content in Fe_xPt_{100-x} thin films. With increasing Fe content, lattice constant c decreases while a increases. The lattice constant a varies in the range of 0.374–0.376 nm while the lattice constant c (or b) varies in the range of 0.369–0.381 nm. The obtained lattice constants of Fe_3Pt thin films grown onto MgO substrates are comparable to the bulk lattice constant value (0.374 nm) [10]. It can be seen that the c decreases a lot comparing to the small increase of the a in this composition range. The c/a ratio is shown in Fig. 4 as a function of Fe composition. It is clearly seen that c/a ratio is increased with decreasing Fe content. This means that

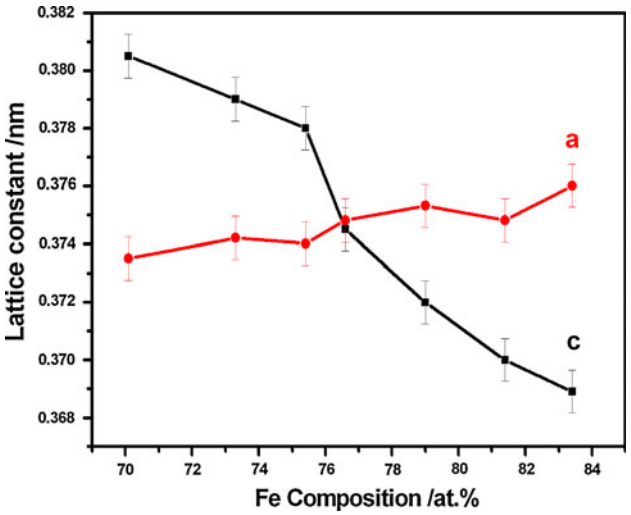

Fig. 3 Changes of lattice constants a and c as a function of Fe contents in ordered Fe_3Pt thin films

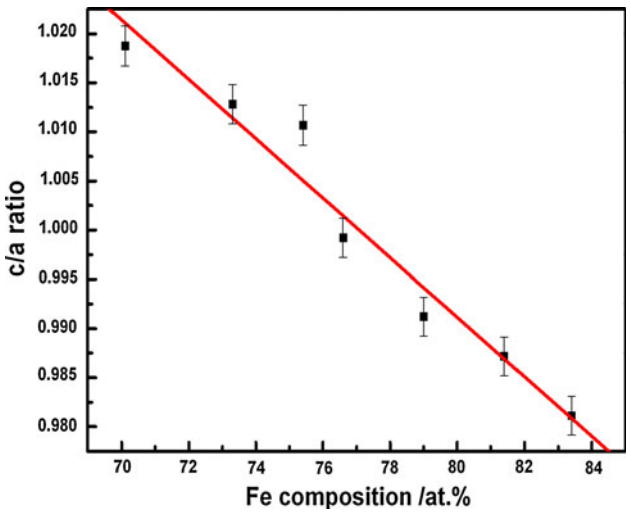

Fig. 4 Lattice constant ratio c/a of Fe_3Pt alloy thin films as a function of Fe composition

when Pt content increases, the Fe_3Pt unit cell is mainly expanded in c-axis direction while there is a small shrinking in a-axis direction.

Magnetic properties

The evolution of magnetic properties resulting from the Fe_3Pt thin films with different Fe contents can be best followed by an examination of the hysteresis loops (M–H curves). The typical M–H curves in both [100] and [011] directions for Fe_3Pt thin films with different Fe contents are shown in Fig. 5a and d. When Fe content is less than 77 at.%, the squareness (M_r/M_s) (S_{100}) in [100] direction is much larger than the squareness (S_{011}) in [011] direction, which indicates that the magnetic anisotropy along [100] direction in the ordered Fe_3Pt thin films was achieved. While S_{100} is almost the same value as S_{011} for the Fe_3Pt films with Fe content from 79 to 83.4 at.%. The coercivity fields of the $Fe_{83.4}Pt_{16.6}$ thin film in both [100] and [011] directions are less than 0.04 T (= 400 Oersted), indicating that the film is dominated by disordered fcc phase. With decreasing Fe contents, the coercivity fields along [100] direction increases from several hundred Oersted to several thousand Oersted while the change of coercivity fields along [011] direction is not very significant. The increase of coercivity fields along [100] direction is mainly due to the higher chemical ordering in Fe_3Pt thin films with decreasing Fe content. The square M–H curves obtained from these thin films with less Fe contents exhibit an initially sharp reversal, indicative of a nucleation barrier for the formation of the oppositely magnetized domains. For samples with Fe content higher than 79 at.%, the nucleation of the negatively (or oppositely) magnetized domain occurs before the external positive field is reduced to zero, because of the demagnetization field of the sample in the [100] direction. For films with Fe content less than 77 at.%, a higher nucleation barrier is present and the nucleation is delayed until the external field has reached zero and become negative, and is now aiding the sample's demagnetization field.

Figure 6a shows the saturated magnetization, M_s, which changes with Fe content. With increasing Fe content, M_s increases. But there is a negative peak when Fe content is around 79 at.%. This sharp drop in saturation magnetization is known to occur within a narrow range of the Fe–Pt alloy composition of nearly Invar composition (25 at.% Pt) [11, 12]. So far the nature of this phenomenon has not been entirely clarified. It is shown that the disordered fcc structure could be in two spin (ferromagnetic and paramagnetic) states whereas the ordered structure has only a ferromagnetic state. [13] The availability of the paramagnetic state in the disordered structure may possibly suggest an explanation of the above phenomenon for slight excess of Fe content with respect to stoichiometry Pt 25% Fe 75%. Or simply it is because of an Invar behavior. The in-plane magnetic anisotropy constants, K_1 and K_2, of Fe_3Pt alloy thin films are estimated by using $L(\theta) = \left(\frac{1}{4}K_1 + \frac{1}{64}K_2\right)\sin 2\theta + \left(\frac{3}{8}K_1 + \frac{1}{16}K_2\right)\sin 4\theta - \frac{3}{64}K_2 \sin 6\theta$ (where L is torque and θ is the angle between applied magnetic field and the easy axis in the basal plane) based on the two-fold torque curves measured from the films and the relationship between K_1/K_2 and the film composition is shown in Fig. 6b. The values of K_1 (positive) and K_2 (negative) are found to be increased with decreasing Fe content and tend to be saturated when Fe content is less than 75.4 at.%. The saturated K_1 and K_2 values of the Fe_3Pt

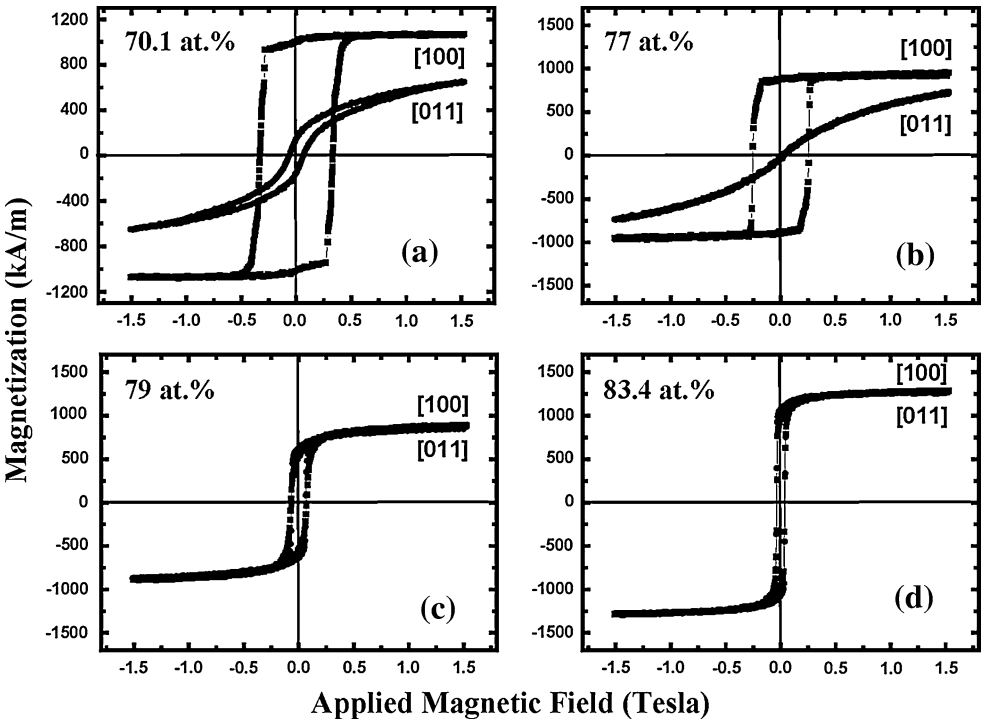

Fig. 5 Typical *M–H* curves in both [100] and [011] directions for Fe_3Pt thin films with different Fe contents

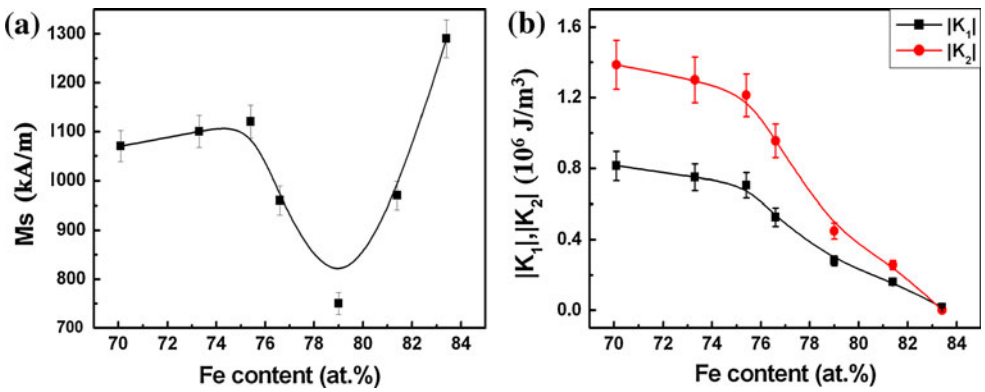

Fig. 6 **a** Saturated magnetization Ms and **b** magnetic anisotropy constants K_1 and K_2 as a function of Fe contents in ordered Fe_3Pt thin films

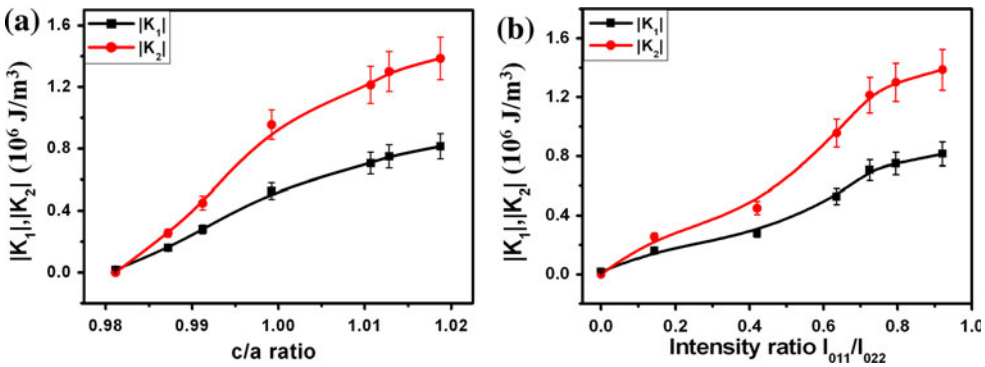

Fig. 7 Relationship between magnetic anisotropy and **a** lattice constant ratio c/a; **b** intensity ratio I_{011}/I_{022} of (011) and (022) peaks

alloy thin films are around 8.2×10^5 and 1.4×10^6 J/m^3, respectively. These values of K_1 and K_2 are much larger than the values of bulk Fe, Ni and comparable to Co [14–16]. Comparing Figs. 4 and 6b), it is observed obviously that the trend of the variation of K_1 and K_2 with Fe composition is similar with the variation *c*/*a*. Figure 7a and b shows the relationships between magnetic anisotropy and lattice constant ratio *c*/*a* and the intensity ratio of the (011) and (022)

peaks of Fe_3Pt phase, respectively. As can be seen from Fig. 7, magnetic anisotropy, K_1 and K_2, increase with increasing *c*/*a* ratio and intensity ratio. This close relationship suggests that the magnetocrystalline anisotropy should be one of the origins of the magnetic anisotropy of the ordered Fe_3Pt alloy thin films. As discussed in Ref. [17], stress-induced magnetic anisotropy is unlikely playing the role of the origin of magnetic anisotropy. Therefore, it might be concluded that the change of magnetic anisotropy in ordered Fe_3Pt thin films with different compositions mainly stems from the magnetocrystalline origin.

Conclusions

The Fe_xPt_{100-x} ($70.1 \leq x \leq 83.4$) thin films with ordered Fe_3Pt phase were grown successfully onto MgO(110) substrates by e-beam co-evaporation technique. The unit cell of ordered Fe_3Pt phase is elongated along *c*-axis direction with decreasing Fe content. The magnetization of thin films shows a negative peak behavior when Fe content is around 79 at.%, which may possibly be due to the availability of the paramagnetic state in the disordered structure or simply because of an Invar behavior. Large in-plane ([100] direction) magnetic anisotropy constants K_1 and K_2 (in the order of 10^6 J/m^3) was obtained when Fe content is around 70–75 at.%. The relationship between magnetic anisotropy and structural parameters suggests that the change of magnetic anisotropy in ordered Fe_3Pt thin films with different compositions most likely stems from the magnetocrystalline origin.

Acknowledgements The present work was supported by National Natural Science Foundation of China (Grant No. 50901052) and Program for Young Excellent Talents in Tongji University (Grant No. 2009KJ003) and "Chen Guang" project (Grant No.10CG21) supported by Shanghai Municipal Education Commission and Shanghai Education Development Foundation.

References

1. Ivanov OA, Solina LV, Demshina VA, Magat LM (1973) Fiz Met Metalloved 35:81
2. Podgorney M (1991) Phys Rev B 43:11300
3. Kim KJ, Lee SJ, Wiener TA, Lynch DW (2001) J Appl Phys 89:244
4. Duplessis RR, Stern RA, MacLaren JM (2004) J Appl Phys 95:6589
5. Nahid MA, Suzuki T (2004) Appl Phys Lett 85:4100
6. Hsiao SN, Chen SK, Hsu YW, Yuan FT, Huang HW, Chin TS, Chang WC, Lee HY (2008) IEEE Trans Magn 44:3902
7. Kakeshita T, Takeuchi T, Fukuda T, Tsujiguchi M, Saburi T, Oshima R, Muto S (2000) Appl Phys Lett 77:1502
8. Sumiyama K, Shiga M, Morioka M, Nakamura Y (1979) J Phys F 9:1665
9. Kakeshita T, Takeuchi T, Fukuda T, Saburi T, Oshima R, Muto S, Kishio K (2000) Mater Trans JIM 41:882
10. Okamaoto H (1993) Phase diagram of binary iron alloys. American Society Metals, Metals Park, OH, p 330
11. Graf L, Kussmann A (1935) Phys Zeit 36:544
12. Kussmann A, von Rittberg GG (1950) Ann Phys 7:173
13. Baldokhin YV, Kolotyrkin PY, Petrov YI, Shafranovsky EA (1997) J Appl Phys 82:3042
14. Gengnagel H, Hofman H (1968) Phys Status Solidi 29:91
15. Franse JJM, de Vries G (1968) Phys Amsterdam 39:477
16. Takahashi M, Suzuki T (1979) Jpn J Appl Phys 18:1071
17. Nahid MAI, Suzuki T (2005) J Appl Phys 97:10K307